

11-1-2010

Enhanced Electrochemistry of Nanoparticle-Embedded Polyelectrolyte Films: Interfacial Electronic Coupling and Distance Dependence

Callie E. Dowdy

Michael C. Leopold

University of Richmond, mleopold@richmond.edu

Follow this and additional works at: <https://scholarship.richmond.edu/chemistry-faculty-publications>

 Part of the [Inorganic Chemistry Commons](#)

This is a pre-publication author manuscript of the final, published article.

Recommended Citation

C.E. Dowdy* and M.C. Leopold, "Enhanced Electrochemistry of Nanoparticle-Embedded Polyelectrolyte Films: Interfacial Electronic Coupling and Distance Dependence," *Thin Solid Films* 2010, 519, 790-796.

This Post-print Article is brought to you for free and open access by the Chemistry at UR Scholarship Repository. It has been accepted for inclusion in Chemistry Faculty Publications by an authorized administrator of UR Scholarship Repository. For more information, please contact scholarshiprepository@richmond.edu.

**Enhanced Electrochemistry of Nanoparticle-Embedded Polyelectrolyte Films:
Interfacial Electronic Coupling and Distance Dependence**

Callie E. Dowdy and Michael C. Leopold*

*Department of Chemistry, Gottwald Center for the Sciences, University of Richmond
Richmond, VA 23173*

Abstract

Factors affecting the electronic communication believed to be responsible for the enhanced solution electrochemistry observed at electrodes modified with hybrid polyelectrolyte-nanoparticle (PE-NP) film assemblies were systematically investigated. Specifically, the faradaic current and voltammetric peak splitting recorded for cyclic voltammetry of ferricyanide redox species ($\text{Fe}(\text{CN})_6^{3/4-}$) at films constructed with various architectures of citrate-stabilized gold NPs embedded in polyelectrolyte films composed of poly-L-lysine and poly-S-styrene was used to establish the relative importance of both distance and electronic coupling. Layer-by-layer construction of PE-NP films allowed for the position and density of NPs to be varied within the film to assess electronic coupling between particles (interparticle coupling) as well as at the electrode-film interface. The cumulative results observed at these films suggest that, while distance dependence prevails in nearly every case and interparticle coupling can contribute to facilitating the $\text{Fe}(\text{CN})_6^{3/4-}$ electrochemistry, interfacial electronic coupling of the PE-NP films is of critical importance and that decoupling is easily achieved by disengaging NP-electrode interactions.

Keywords: polyelectrolyte, nanoparticles, electrochemistry, interfacial coupling, voltammetry

*To whom correspondence should be addressed. Email: mleopold@richmond.edu. Phone: (804) 287-6329. Fax: (804) 287-1897

Introduction

Thin films of composite materials involving nanoparticles (NPs) are of interest as surface coatings or ultrathin devices with purposefully engineered functionality. Hybrid materials of this nature that incorporate metallic NPs are of particular interest because of their potential to offer controllable electronic and/or optical properties [1-4]. An important type of material in this area of research is polymer films that are embedded with nanostructures. Assemblies of multi-layered polyelectrolyte (PE) films constructed with the specific inclusion of metal nanospheres [1-7] or nanoshells [7] have been investigated as a nanocomposite interface with potential applications in catalysis, biocompatibility and biosensor technology, and membrane development for both separation science as well as charge storage [2,8-9].

In many cases, research involving the use of NPs as part of an electrochemical interface has shown an “enhancement” or significant improvement to the observed electrochemistry that is directly attributed to the presence of the NPs within the films. For example, Ulstrup and coworkers [10] describe a gold nanoparticle-assisted enhancement of long range electron transfer (ET) of over 50 Å between an electrode and adsorbed heme protein cytochrome c (cyt c). The long range ET is observed only for systems where cyt c is directly adsorbed to an immobilized layer of carboxylic acid functionalized gold nanoparticles at the electrode surface, a configuration which results in a reported order of magnitude increase in the ET rate constant compared to the same system without the NPs. In our own laboratory [11-12], we have observed the lack of traditional distance dependence for ET of the proteins azurin and cyt c adsorbed to multi-layer assemblies of alkanethiolate monolayer protected nanoclusters. While no enhancement is seen, our experiments show a nearly negligible decay in the ET rate over distances up to 20 nm [12]. In both our work [11] as well as in Ulstrup’s [10] study, the observed

enhancement of ET kinetics at NP films was attributed to an improved electronic coupling of the adsorbed protein to the electrode via highly efficient ET conduits provided by the NPs. In other work by Li et al. [13], electrodes modified with multi-layers of DNA functionalized NPs are shown to amplify the electrochemical signal of adsorbed cyt c with significant improvement of voltammetric peak definition as well as a two-fold increase in ET rate constant. Their report also suggests that voltammetry of the ferricyanide redox couple ($\text{Fe}(\text{CN})_6^{3/4}$) in solution is facilitated by a greatly improved electronic communication with the electrode provided by the NP film assembly. The effect of the NP film on solution $\text{Fe}(\text{CN})_6^{3/4}$ electrochemistry is described as dominant, where as the number of NPs within the film is increased, there is a corresponding drop observed in the interfacial resistance. In most of these studies, the electrochemical enhancement recorded with the incorporation of NPs as an interfacial material has been attributed, in some manner, to the NPs acting as an effective conduit or relay that facilitates ET reactions of solution redox species.

Important work in this area is that of Fermin and coworkers, [3,14-15] where the nanoparticle-mediated ET across hybrid films of polyelectrolyte (PE) and NPs was studied. In a series of investigations aimed at electrochemical aspects of multi-layer films of PE (positively charged poly-L lysine and negatively charged polyglutamic acid) that are subsequently augmented with gold NPs at the film/solution interface, Fermin et al. have indicated several findings of interest. In early work [3], Fermin reports that the addition of NPs at the outer layer of a PE film has a dramatic effect on the electrochemistry of $\text{Fe}(\text{CN})_6^{3/4}$ in solution. Traditional blocking behavior of the PE film toward $\text{Fe}(\text{CN})_6^{3/4}$ is easily overcome with the addition of the NPs at the film/solution interface, including a decrease in peak splitting (faster ET kinetics) coupled with an increase in current density that suggests an unhindered electron exchange

reaction between the NP and electrode (i.e., $\text{Fe}(\text{CN})_6^{3/4-}$ voltammetry at the NP/PE film nearly behaves as if it were at a bare gold electrode). A subsequent report by Fermin [14] examined the effect of adding NPs to the periphery of PE films of varying thickness, determining that the charge transfer resistance of the NP-embedded films is two orders of magnitude lower than that of PE films without NPs and that the ET kinetics appear independent of the number of PE layers up to film thicknesses of 6.5 nm as measured via AFM. In similar work [15], Fermin's lab investigated the ability of PE/NP composite films to overcome the ET blocking behavior of self-assembled monolayers (SAMs). Voltammetry of $\text{Fe}(\text{CN})_6^{3/4-}$ at SAM-modified electrodes shows progressive blocking behavior with increasing numbers of SAM methylene units. Fermin, performing the same experiment at NP/PE/SAM systems, revealed $\text{Fe}(\text{CN})_6^{3/4-}$ voltammetry indistinguishable from that at bare gold when the anchoring SAM incorporates fewer than 5 methylene units (CH_2) and faradaic current that, while attenuated, is independent of chain length ($\geq 5 \text{ CH}_2$). This collection of results by Fermin and coworkers [1, 14-15] suggests a significant and long range electronic communication between the metal electrode and the metallic NPs incorporated into the PE film assembly. The apparent "unhindered" ET kinetics Fermin observes in the electrochemistry at these NP-PE films is explained as an effect associated with the film's partial permeability toward solution redox species that become trapped within the PE layers of the film.

In the work reported here, we probe the critical factors in the electronic communication of these hybrid PE – NP film composites that lead to the electrochemical enhancements of solution redox species reported by others [3, 14-15]. The voltammetry of ferricyanide ($\text{Fe}(\text{CN})_6^{3/4-}$) at film assemblies anchored with a self-assembled monolayer (SAM) of 11-mercaptopundecanoic acid (MUA) and augmented with polyelectrolyte bilayers of cationic poly-

L-lysine (PLL) and anionic poly-S-styrene that are subsequently impregnated with citrate-stabilized gold nanoparticles (CSNPs) are explored in detail. Unlike previous work on these materials, our study involves the systematic variation of the location and number of NP layers within the film to evaluate the importance of film-electrode, film-solution, and interparticle electronic coupling in heterogeneous electron transfer (ET) reactions, including films with single, double and multi-layers of embedded NPs. The apparent ET kinetics from voltammetric measurements are used as a guide for determining the importance of NP placement within the films as well as establishing the relative importance of electronic coupling and the distance dependence of ET in the various NP-PE film systems.

Experimental Details

All materials and chemicals were purchased from Sigma Aldrich unless otherwise stated. CSNPs were synthesized using well-established procedures [16] developed by Natan and coworkers [17-19]. Briefly, 250 mL of aqueous 1 mM HAuCl₄ was heated to 100°C with constant stirring in a flask attached to a reflux condenser, and 25 mL of a 38.8 mM sodium citrate solution was added immediately when the solution boiled. The solution changed from a pale yellow color to clear to a deep burgundy. The solution was allowed to continue to reflux for ten minutes, then removed from heat and allowed to cool to room temperature with continued stirring. The solution was vacuum filtered using a 1 mm filter (Gilman) and the resulting filtrate was stored in an opaque container at room temperature until further use. The nanoparticles were routinely characterized with UV-Vis spectroscopy (Agilent) and transmission electron microscopy and found to have a well-defined surface plasmon band at 510 nm and an average diameter of 9-10 nm respectively, consistent with prior research [16-19].

Multi-layer PE films were grown via a previously reported layer-by-layer procedure on a gold electrode (Evaporated Metal Films, Inc.) after it had been electrochemically cycled [16,20] in a solution of 0.1 M sulfuric acid and 0.01 M potassium chloride. This clean gold electrode was immersed in a 5 mM ethanolic solution of mercaptoundecanoic acid (MUA) for 48 hours to form a carboxylic acid terminated self-assembled monolayer (SAM) exposing carboxylate groups at the solution interface. The SAM-modified gold electrode was then exposed to an aqueous solution (1 mg/mL) of the cationic PE poly-L-lysine (PLL) for 20 minutes before being rinsed with copious amounts of water and subsequently exposed to an aqueous solution of anionic PE poly-S-styrene (PSS) for 20 minutes. Multi-layer films of varying thickness were created by alternating these procedures for PLL and PSS in succession to create an electrostatically assembled film between positive and negative charged PEs. During film growth, CSNP were embedded into the PE films at different points by interrupting the alternating procedure after a PLL exposure (positively charged PE) and exposing the film to a solution of CSNPs for 2 hours [21]. A schematic example of a PE-NP film construction is provided in **Figure 1**, where we have designated the “**n unit**” as a PLL/PSS bilayer and the “**m unit**” as the PLL/CSNP augmentation layer.

Cyclic voltammetry was performed with CH Instruments potentiostat (Model 420A) and was used to electrochemically monitor layer-by-layer growth at each stage of film construction within an electrochemical “sandwich” cell equipped with an Ag/AgCl (satur. KCl) reference electrode, a platinum wire counter electrode, and a gold working electrode (0.32 cm²) defined by a viton o-ring [11,16,22]. The voltammetry of a 5 mM solution of the ferricyanide redox couple probe (Fe(CN)₆^{3+/4-}) in 0.5 M KCl supporting electrolyte was examined by scanning the potential window of -0.2 to 0.6 V at 100 mV/sec versus the reference electrode. Cyclic voltammetry

experiments were performed with a minimum of 6 cycles to ensure the stability and repeatability of the signal over time before the final complete cycle was utilized for comparisons and to display results. For the purposes of generating graphical representations of the data collected from these experiments, some results were quantified by determining the current flow at the anodic peak potential (E_{pa}) of $\text{Fe}(\text{CN})_6^{3/4-}$ at bare gold electrodes ($E_{pa} = 0.3 \text{ V vs. Ag/AgCl (KCl)}$) for the tested film systems. Potential peak splitting (ΔE_p) between the anodic (ΔE_{pa}) and cathodic (ΔE_{pc}) voltammetric waves was used as a semi-quantitative measure of ET kinetics. Standard deviation of measurements were calculated with a minimum of three measurements on individual experiments involving independent film systems.

Results and Discussion

The potassium ferricyanide redox couple, $\text{Fe}(\text{CN})_6^{3/4-}$, can be used as a solution probe of electrochemical activity at an interface. Current attenuation and increases in peak splitting of the $\text{Fe}(\text{CN})_6^{3/4-}$ voltammetry, for example, are examples of slower ET kinetics - a common occurrence as the electrode interface is effectively blocked with a modifier. This type of blocking behavior at a SAM-modified electrode is clearly illustrated in Figure 2, where diffusional voltammetry of $\text{Fe}(\text{CN})_6^{3/4-}$ at a bare gold electrode versus a carboxylic acid terminated SAM (MUA) is directly compared. As shown, the complete blocking of the redox probe produced by the SAM interface is evident. The lack of voltammetry observed at the SAM is likely assisted by electrostatic repulsion between the $\text{Fe}(\text{CN})_6^{3/4-}$ and the SAM's carboxylic acid endgroups. The addition of the polyelectrolyte, PLL, at the interface causes a minimal increase in faradaic current associated with the redox probe $\text{Fe}(\text{CN})_6^{3/4-}$ at the edges of the potential window, most likely the result of the altered electrostatic environment which sensitizes the redox probe to film defects [3]. With the

adsorption of CSNPs (2 hour exposure) to the film interface, the voltammetry of $\text{Fe}(\text{CN})_6^{3/4-}$ is restored and approaches the response observed at bare gold, indicating that the NPs can facilitate the ET reaction through the existing SAM barrier. This “enhancement” behavior is consistent with what has been observed in the literature when NPs are introduced to PE-SAM interfaces – an apparent unhindered ET reaction of a solution redox species [3, 23].

To investigate the effect of film thickness (distance) on the voltammetric “enhancement” observed with a PE film terminated with a single layer of NPs at the interface, $\text{Fe}(\text{CN})_6^{3/4-}$ redox probing was performed on film systems where the number of PE layers between the MUA SAM and the layer of CSNPs was systematically increased. UV-Vis spectroscopy of similar PE-NP hybrid film assemblies grown with the procedures described in this study indicate that the film assembly proceeds in a layer-by-layer fashion, with each exposure to PE or NP yielding a corresponding increase in absorbance – evidence for material building up on the substrate and increased film thickness [6-7,16-19]. Cyclic voltammograms of polyelectrolyte films of various thicknesses are shown in **Figure 3A-E**, where n is defined as the number of $(\text{PLL-PSS})_n$ polymer bilayers between the gold electrode and the terminal PLL-CSNP layer (i.e., the n unit and the m unit shown in Figure 1, respectively). The results of **Figure 3** compare the voltammetry of $\text{Fe}(\text{CN})_6^{3/4-}$ at the PE-NP composite film as well as at the same film without NPs and at bare gold. It is evident from the results that, as the number of polymer layers between the electrode and CSNPs increases, there are corresponding dramatic decreases in the maximum current flow through the film (I_p) and increases in peak splitting (ΔE_p), both indicators of slower ET kinetics. This result is consistent with a voltammetric description of an electrode that is becoming increasingly blocked by increasing numbers of polymer layers. This result is significant since it suggests that despite initial voltammetric “enhancement” observed when CSNPs are adsorbed

close to the surface of a SAM-modified gold electrode, this benefit diminishes as the adsorbed NP layer is moved further away and is decoupled from the electrode, even if that separation is due to the presence of PE layers with low resistivity [14-15].

The collective quantitative analysis of the voltammetry shown in Figure 3A-E is shown in Figure 3F and emphasizes the different measured currents of the PE films constructed with and without CSNPs. For comparison, the current measurements of $\text{Fe}(\text{CN})_6^{3/4-}$ at bare gold and gold modified with a SAM-PLL layer are also included at $n=0$, the maximum and minimum current flow through the film, respectively. From the results, one can observe a distinct elevation of current for films including CSNPs compared to those that do not. However, it is also evident that this enhancement of current is a distance dependant effect where, after 10 PE bilayers of separation, the current converges to match that of a film without CSNPs. Using AFM to measure the depth profile of these same PE assembled films, Fermin [14] was able to estimate a thickness of 0.65 nm/bilayer or 6.5 nm for 10 bilayers[24,25] - the same distance or thickness of the PE bilayers separating the NPs from the SAM-modified electrode in our Figure 3F results. Collectively, these results suggest that the electronic benefit of the incorporated NPs has a limited range and that distance dependence perseveres since increasing the number of PE layers in the film system effectively “decouples” the terminal NP layer from the electrode.

To further investigate the role of NPs in the voltammetric enhancement, films containing two independent layers of CSNPs, one closely coupled to the electrode and the other at the film/solution interface, separated by increasing numbers of polyelectrolyte layers were tested. The specific film composition is indicated as the following: $[\text{Au-MUA-(PLL-CSNP)}_{m=1}-(\text{PLL-PSS})_{n=1, 3, 5, 7 \text{ or } 10}-(\text{PLL-CSNP})_{m=1}]$, where there are two m units separated by varying numbers of PE bilayers (n). The electrochemistry of $\text{Fe}(\text{CN})_6^{3/4-}$ at these type of “double NP layer” films has not

been previously reported, and the addition of a layer of CSNPs close to the electrode surface could provide insight into the importance of electronically coupled NPs role in the “enhancement” of the voltammetry of solution redox species. As illustrated in the results shown in Figure 4, current flow from the voltammetry of solution $\text{Fe}(\text{CN})_6^{3+4}$ at the double NP layer films remains elevated well above the same films constructed with only SAM-PE layers (i.e., no CSNPs). However, the voltammetry with increasing number of PE bilayers separating the layers of CSNPs clearly indicates that this current enhancement remains distant dependent where, at 10 bilayers of separation or ~ 6.5 nm[14], it eventually diminished to current levels nearly identical to that achieved at PE films void CSNPs (Figure 4C). From the voltammograms recorded for $\text{Fe}(\text{CN})_6^{3+4}$ at these films as a function of increasing the thickness of the PE barrier between the layers increasing CSNPs (Figure 4A,B) there is also a systematic decrease in the apparent ET kinetics, as evidenced by increased ΔE_p . Taken together, these trends again suggest that as separation distance increases, the NP composite film again becomes decoupled from the electrode. Remarkably, in spite of the fact that insertion of a second layer of CSNPs approximately doubles the thickness of the films[14,26], the voltammetric current from the $\text{Fe}(\text{CN})_6^{3+4}$ in solution is nearly the same as the current recorded at the single NP films studied in Figure 3. For example, if one compares three-bilayer ($n=3$) films consisting of only an outer layer of NPs (Figure 3) to the double film with both an inner and outer layer of NPs, the current measured is very similar ($\sim 150 \mu\text{A}$) even though the overall film thicknesses are estimated at 12 and 22 nm, respectively. Thus, the results suggest that even though the redox interface for $\text{Fe}(\text{CN})_6^{3+4}$ is much further away from the electrode in the double NP layer films, the film is still able to facilitate $\text{Fe}(\text{CN})_6^{3+4}$ electrochemistry to nearly the same degree, an indication that while distance may remain as the ultimate limitation for electronic communication through the hybrid

NP-PE films, they are also clearly also significantly influenced by interparticle electronic coupling.

In light of the previous results presented that indicate that interparticle electronic coupling may be a contributing factor to the observed electrochemical enhancement, multilayer films of NPs layered with minimal PE separation layers were explored. Since a single layer of CSNPs close to the electrode surface was found to enhance the voltammetry of an electrode blocked by a MUA SAM (Figure 3) and interparticle coupling appears to be a factor (Figure 4), it was hypothesized that multiple layers of CSNPs in close proximity to the electrode and to one another would promote enhanced ET kinetics over a significant film thickness. To test this concept, films featuring multiple consecutive layers of CSNPs separated with only single PLL layers (i.e., repeating m units with no PSS layers) were constructed at MUA SAM modified electrodes (see schematic inset Figure 5A). Thus, in these experiments, m refers to the number of PLL-CSNP layers in the film, for an overall film construction notation of [Au-MUA-(PLL-CSNP) _{$m=1, 3, 5, 7$ or 10}]. It should be noted that these films, with each layer of NPs being approximately 10 nm thick (single PLL linking layers estimated at 0.3 nm[14,24,25]), represent some of the thickest films tested. The results of Fe(CN)₆^{3-/4-} voltammetry experiments utilizing these multilayer CSNP films are shown in Figure 5A and show the overall kinetics of ET have distance dependence but also a significant flow of current compared to other films tested. Interestingly, these multi-layer NP films sustained a significantly higher faradaic current with substantially faster ET kinetics for solution Fe(CN)₆^{3-/4-} voltammetry compared to much thinner films incorporating only single layer of NPs or “double layer” NP films in which the NPs are separated by PE layers. For example, the thickest multi-layer films ($m=10$) which are estimated to be approximately exhibited greater current flow than much thinner ($n \geq 5$) single NP layer films and

nearly all of the double layer NP films, further suggesting a general increase in conductivity through multi-layer films facilitated by interparticle coupling, which is absent in single layer films. Also observed in these experiments was the consistent and repeatable increase in current between adding the first and second layers of NPs ($m=1, 2$), an enhancement attributed to interparticle and film/electrode coupling that is noticeably absent from corresponding experiments on films without NPs (not shown). Beyond the second layer of NPs, however, the voltammetry reflects peak splitting traditional for a successively blocked electrode.

To illustrate the comparisons between the different types of film systems, Figure 5B presents the apparent ET kinetics, measured as the voltammetric peak splitting or ΔE_p , of all the film systems in our study as a function of their thicknesses, either PE bilayers (n) at 0.65 nm/bilayer or units of PLL-CSNPs (m) at 10.3 nm/ m unit. It is easily observed in this comparison that the multilayer films (system a) facilitate the fastest ET kinetics (smallest ΔE_p), an indication that interparticle electronic coupling in these films can be a significant contributor to the ET through the film even at very thick multi-layer NP films. The single NP layer films, those with polyelectrolyte layers separating electrode and NPs (system b), have similar ET kinetics compared to the multi-layer films up to a point. As seen in the figure, there is a rather abrupt change in the ΔE_p between 5 and 7 bilayers of PE separation, indicating that, at a defined distance, the NPs clearly become decoupled from the electrode and the enhancement due to their presence is minimized. A similar pattern of apparent ET kinetics is achieved with the double NP layer films (system d) which emphasizes interparticle electronic coupling that may be able to overcome larger ET distances. Experimentation with an inverted single NP layer system, where NPs coupled to the electrode surface are effectively buried under PE layering (system c) possessed the slowest ET kinetics of any tested films. The distinct difference in kinetics between

this system, the only one to not have NPs embedded at the outer layer of the film, and the other systems may be a signal that electronic coupling at the film-*solution* may, in addition to film-electrode coupling, be important. More importantly, these collective results suggest that PE layers of significant thickness can be used to disengage the NP facilitated electronic coupling to the electrode and/or the interparticle electronic interactions and effectively “turn off” the electrochemical enhancement. This phenomenon of decoupling the film was further explored with multi-layer NP films as described below.

With the establishment that interparticle coupling has a significant influence on the voltammetric enhancement observed for solution redox species at these films, the importance of interfacial coupling in the presence of interparticle coupling was evaluated. To do this, the multi-layer NP films with the highest ET kinetics were again targeted. In an attempt to decouple the NP assembly from the electrode, multi-layer films were altered by removing the first two layers of NPs closest to the electrode, replacing them with PSS polymer layers for an overall film construction of [Au-MUA-(PLL-PSS)_{m=2}-(PLL-CSNP)_{m=1, 2, 3, 5, 7, or 8}]. Measuring the peak splitting of Fe(CN)₆^{3/4-} voltammetry at these replaced films and comparing the results to multi-layer films with conductive NP layers close to the electrode still intact illustrates the critical nature of interfacial coupling at the electrode. As shown in **Figure 5C**, multi-layer PLL-NP films with the first two layers of CSNPs replaced with PSS have a substantially different trajectory of ET kinetics as the film is made thicker with additional layers (increasing m). With the “decoupling” of the film via the removal of NPs close to the electrode interface, the ET kinetics of Fe(CN)₆^{3/4-} are decidedly sensitive to distance, displaying a more abrupt increase in the ΔE_p . For example, after the third layer is assembled (m=3) the difference in ΔE_p for Fe(CN)₆^{3/4-} voltammetry at electronically coupled versus decoupled (PSS replaced) multi-layer NP films is nearly 150 mV

even though the films are of similar thickness [27]. These results support the notion that the electrochemical enhancement observed with any of these NP-PE hybrid films is highly dependent on effective NP coupling at the electrode/film interface regardless of contributions from interparticle coupling throughout the film.

Conclusions

The electrochemistry of $\text{Fe}(\text{CN})_6^{3/4-}$ at various polyelectrolyte films featuring different NP positions and densities has been used to delineate factors affecting the electrochemical enhancement observed with films of these constructs [3, 10-12, 14-15]. Our results suggest that this enhancement effect is markedly distance dependent but is also inherently linked to the degree of electronic communication within the film assembly. Electronic coupling of the hybrid NP film at the electrode interface is of critical importance as the results of our study show films can be effectively decoupled from the electrode via spacing or insulating of the NP from the interface regardless of the conductive nature of the separating medium. This concept of decoupling electronic communication in nanoparticle films is consistent with reports of other nanoparticle systems as well [14-15]. In our lab [12], we have examined the ET reaction of proteins adsorbed to film assemblies comprised of nonaqueous alkanethiolate protected nanoparticles and observed that there was very little distance dependence of the ET rate constant – an effect that is negated if the NP film is anchored at the electrode interface with a SAM of substantial chainlength, effectively decoupling the film. Here, substantial electronic coupling of these films is achieved with minimizing separation of NPs nearest to the electrode (interfacial electronic coupling) and, to a lesser degree, by constructing films that take advantage of inter-particle electronic interactions. In our studies, films with significant electronic coupling of this nature exhibit faster apparent ET kinetics and/or inflated sustained current flow compared to similar systems void of

NPs. The overwhelming dominant factors in the PE-NP films, however, are the distance and electronic coupling of NPs to the electrode interface. Additionally, this study establishes that the electronic properties of nanocomposite films, such as those studied here, can be readily manipulated by specific engineering of the electrode/film interface, controlling interparticle distances and density as well as the film's anchoring layer. Understanding electronic communication in these hybrid material films is important for continued development of electronically sensitive nanoscale devices and coatings [1-4].

Acknowledgements

We gratefully acknowledge the National Science Foundation (CHE-0847145) and the Arts & Sciences Faculty Research Committee for generously supporting this research. We also would like to specifically recognize Robert Day, Anne Galyean, and Tran Doan for their important contributions to this project. Special thanks is given to Drs. Tamara Leopold, Rene Kanters, Diane Kellogg, Rob Miller and Will Case, as well as Russ Collins, Phil Joseph, Mandy Mallory, and John Wimbush - all of whom make undergraduate research possible at the University of Richmond. A very personal thank you is given to Lauren Leopold.

References

- [1] J. Schmitt, G. Decher, W. Dressick, S. Brandow, R. Geer, R. Shashidhar, J. Calvert, J. Adv. Mater. 9 (1997) 61.
- [2] J. Jeon, V. Panchagnula, J. Pan, A. Dobrynin, Langmuir 22 (2006) 4629.
- [3] J. Zhao, C. Bradbury, S. Huclova, I. Potapova, M. Carrara, D. Fermin, J. Phys. Chem. B 109 (2005) 22985.
- [4] R. Chapman, P. Mulvaney, Chem. Phys. Lett. 349 (2001) 358.
- [5] P. Mulvaney, Langmuir 12 (1996) 788.
- [6] M. Chirea, V. García-Morales, J.A. Manzanares, C. Pereira, R. Gulaboski, F. Silva, J. Phys. Chem. B 109 (2005) 21808.
- [7] A. Galyean, R. Day, J. Malinowski, K. Kittredge, M. Leopold, J. Colloid Interface Sci. 331 (2009) 532.
- [8] H. Santos, M. Chirea, V. García-Morales, F. Silva, J. Manzanares, K. Konturri, J. Phys. Chem. B 109 (2005) 20105.
- [9] R. Gulaboski, M. Chirea, C. Pereira, M. Cordeiro, D. Natália, R. Costa, F. Silva, J. Phys. Chem. C 112 (2008) 2428.
- [10] P. Jensen, Q. Chi, F. Grumsen, J. Abad, A. Horsewell, D. Schiffrin, J. Ulstrup, J. Phys. Chem. C 111 (2007) 6124.
- [11] A. Loftus, K. Reighard, S. Kapourales, M. Leopold, J. Am. Chem. Soc. 130 (2008) 1649.
- [12] M. Vargo, C. Gulka, J. Gerig, C. Manieri, J. Dattelbaum, C. Marks, N. Lawrence, M. Trawick, M. Leopold, Langmuir 26 (2010) 560.
- [13] J. Zhao, X. Zhu, T. Li, G. Li, Analyst 133 (2008) 1242.
- [14] J. Zhao, C. Bradbury, D. Fermín, J. Phys. Chem. C 112 (2008) 6832.
- [15] C. Bradbury, J. Zhao, D. Fermin, J. Phys. Chem. C 112 (2008) 10153.
- [16] L. Russell, A. Galyean, S. Notte, M. Leopold, Langmuir 23 (2007) 7466.
- [17] M. Musick, C. Keating, M. Keefe, M. Natan, Chem. Mater. 9 (1997) 1499.
- [18] L. Lyon, D. Pena, M. Natan, J. Phys. Chem. B 103 (1999) 5826.

- [19] M. Musick, C. Keating, L. Lyon, S. Botsko, D. Pena, W. Holliway, T. McEvoy, J. Richardson, M. Natan, *Chem. Mater.* 12 (2000) 2869.
- [20] J. Hoogvliet, M. Dijkstra, B. Kamp, W. Van Bennekom, *Anal. Chem.* 72 (2000) 2016.
- [21] Both Li [13] and Fermin et al. [3, 14-15] note that electrochemical enhancement effects are increased with time exposure to NPs up to 30 minutes. In this respect, we have chosen to maximize potential effects by eliminating adsorption time dependence, exposing films to NP solutions for 2 hours.
- [22] L. Russell, R. Pompano, K. Kittredge, M. Leopold, *J. Mater. Sci.* 42 (2007) 7100.
- [23] It should be noted that Fermin and coworkers use the negatively charged polyelectrolyte polyglutamic acid (PGA) in their film systems [3, 14-15], whereas these experiments use poly-S-styrene. However, the experiments detailed in the following experiments were repeated with PGA, with no significant difference in the results (not shown).
- [24] Fermin's measurement of the thickness of polyelectrolyte (PLL-PGA) bilayers is in agreement with surface plasmon resonance measurement of PLL-PGA films by Cheng and Corn [25].
- [25] Y. Cheng, R. Corn, *J. Phys. Chem. B* 103 (1999) 8726.
- [26] For example, our own measurements and that of Natan's group have characterized the CSNPs as having an average diameter of approximately 10 nm [16-19] while Fermin and coworkers estimate that each polyelectrolyte bilayer is approximately 0.65 nm thick. Thus, for a single NP layer and double NP layer with three bilayers ($n=3$), film thickness beyond the SAM would be estimated at ~12 nm and ~22 nm, respectively. We note that the SAM thickness, because it is the same for all the films constructed, is not included as part of the film thickness estimations.
- [27] Using Fermin's estimates [14], the thickness of the films at $m=3$ in Figure 5C can be calculated. The multi-layer film has 3 layers of NPs at 10 nm each, separated by PLL linkage layers at 0.3 nm each for a total film thickness of ~30 nm. Similarly, the film constructed with additional layers of PE at the electrode interface would have 3 layers of NPs at 10 nm each, separated by PLL linkage layers at 0.3 nm each, and the 2 PE bilayers at the electrode interface at 0.65 nm each for a total film thickness of ~32 nm.

Captions

Figure 1. Schematic of electrostatically assembled polyelectrolyte (PE) – citrate-stabilized nanoparticle (CSNP) composite films anchored with a carboxylic acid terminated self assembled monolayer (MUA-SAM) and subsequently modified with bilayers (n units) composed of poly-L-lysine (PLL) and poly-S-styrene (PSS). Negatively charged CSNPs can be introduced into the film assembly at any stage after a PSS layer by subsequently exposing the film to PLL followed by CSNPs (m unit). For the schematic example shown above, there is one n unit and one m unit, indicating the film was constructed with one bilayer of PLL/PSS and capped with PLL/CSNPs for an overall film representation of Au-MUA-(PLL-PSS)_{n=1}(PLL-CSNPs)_{m=1} – a notation that will be used throughout our study.

Figure 2. Cyclic voltammetry of 5 mM ferricyanide in aqueous 0.5 M KCl supporting electrolyte (100 mV/sec) at a bare gold electrode (black, dotted) and a gold electrode modified with a MUA SAM (red, solid), a MUA SAM and an adlayer of PLL (blue, dashed), and a MUA SAM with the PLL adlayer and a terminal layer of CSNPs (green, solid).

Figure 3. (A-E) Cyclic voltammetry of 5 mM ferricyanide in 0.5 M aqueous KCl supporting electrolyte (100 mV/sec) at “single layer” hybrid PE-NP films with a where the number of PE bilayers (n) between the SAM layer and the terminal NP layer is systematically varied between 1 (Figure 3A) and 10 (Figure 3E), a film composition represented by Au-MUA-(PLL-PSS)_{n=1,3,5,7 or 10}(PLL-CSNPs)_{m=1}. For comparison, each set of voltammograms (A-E) contains ferricyanide voltammetry at a bare gold electrode (black, dotted) as well as at a similar PE film constructed without NPs (“no NPs”). (F) Current measurements made at the anodic peak potential (E_{pa}) for ferricyanide as a function of PE bilayers (n) for these films constructed with and without NPs. For comparison, the anodic voltammetric current of ferricyanide at bare gold (x) and at a gold electrode modified with MUA-PLL (O) are included at n=0. In cases where error bars are not readily visible, the error is smaller than the data point marker.

Figure 4. (A) Cyclic voltammetry of 5 mM ferricyanide in 0.5 M aqueous KCl supporting electrolyte (100 mV/sec) at a “double NP layer” hybrid PE-NP films of thickness n=1, for an overall film construction of Au-MUA-(PLL-CSNPs)_{m=1}-(PLL-PSS)_{n=1}-(PLL-CSNPs)_{m=1}. (B) Cyclic voltammetry of 5 mM ferricyanide in 0.5 M aqueous KCl supporting electrolyte (100 mV/sec) at a “double NP layer” hybrid PE-NP films where the number of PE bilayers (n) between NPs close to the electrode at the SAM/film interface and a terminal layer of NPs at the film/solution interface is systematically varied between 1 (Figure 4A) and 10 (Figure 4B), a film composition represented by Au-MUA-(PLL-CSNPs)_{m=1}-(PLL-PSS)_{n=1,3,5,7 or 10}-(PLL-CSNPs)_{m=1}. Each set of voltammograms (A,B) contains ferricyanide voltammetry at a bare gold electrode (black, dotted) as well as at a similar PE film constructed without NPs (“no NPs”). (C) Current measurements made at the anodic peak potential (E_{pa}) for ferricyanide as a function of PE bilayers (n) for these films constructed with and without NPs. For comparison, the anodic voltammetric current of ferricyanide at bare gold (x) and at a gold electrode modified with MUA-PLL (O) are included at n=0. Error bars for the data representing films with no NPs are smaller than the data points themselves.

Figure 5. (A) Cyclic voltammetry of 5 mM ferricyanide in 0.5 M aqueous KCl supporting electrolyte (100 mV/sec) at multilayer CSNP films. In this case, the bare gold electrode (black,

dotted) was modified with consecutive layers (m) of PLL-CSNPs from m=1 (red, solid) to m=10 (pink, solid), for an overall film construction of [Au-MUA-(PLL-CSNP)_{m=1-10}] (not all shown). (B) Graphical representation of ET kinetics in the form of voltammetric peak splitting (ΔE_p) in multi-layer films (system a), single layer NP films (system b), double layer NP films (system c), and inverted single layer NP films (system d), as a function of film thickness (n or m units). (C) Graphical representation of ΔE_p of the multi-layer NP system (blue diamonds) vs. the multi-layer NP system with the first two layers of CSNPs replaced with PSS polymer (red squares), plotted as a function of increasing layers of CSNPs (m).

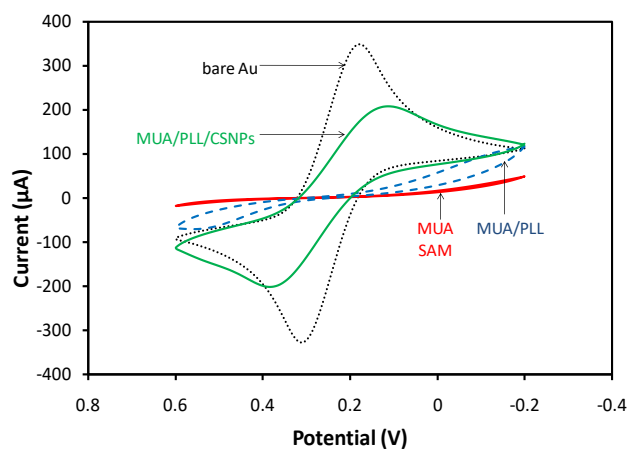


Figure 2. Cyclic voltammetry of 5 mM ferricyanide in aqueous 0.5 M KCl supporting electrolyte (100 mV/sec) at a bare gold electrode (black, dotted) and a gold electrode modified with a MUA SAM (red, solid), a MUA SAM and an adlayer of PLL (blue, dashed), and a MUA SAM with the PLL adlayer and a terminal layer of CSNPs (green, solid).

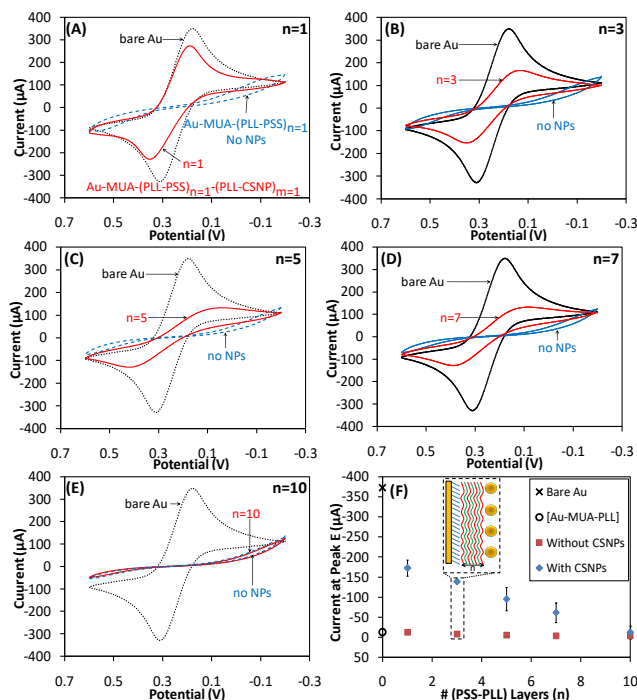


Figure 3. (A-E) Cyclic voltammetry of 5 mM ferricyanide in 0.5 M aqueous KCl supporting electrolyte (100 mV/sec) at “single layer” hybrid PE-NP films with a where the number of PE bilayers (n) between the SAM layer and the terminal NP layer is systematically varied between 1 (Figure 3A) and 10 (Figure 3E), a film composition represented by Au-MUA-(PLL-PSS)_{n=1,3,5,7 or 10}-(PLL-CSNPs)_{m=1}. For comparison, each set of voltammograms (A-E) contains ferricyanide voltammetry at a bare gold electrode (black, dotted) as well as at a similar PE film constructed without NPs (“no NPs”). (F) Current measurements made at the anodic peak potential ($E_{p,a}$) for ferricyanide as a function of PE bilayers (n) for these films constructed with and without NPs. For comparison, the anodic voltammetric current of ferricyanide at bare gold (x) and at a gold electrode modified with MUA-PLL (O) are included at n=0. In cases where error bars are not readily visible, the error is smaller than the data point marker.

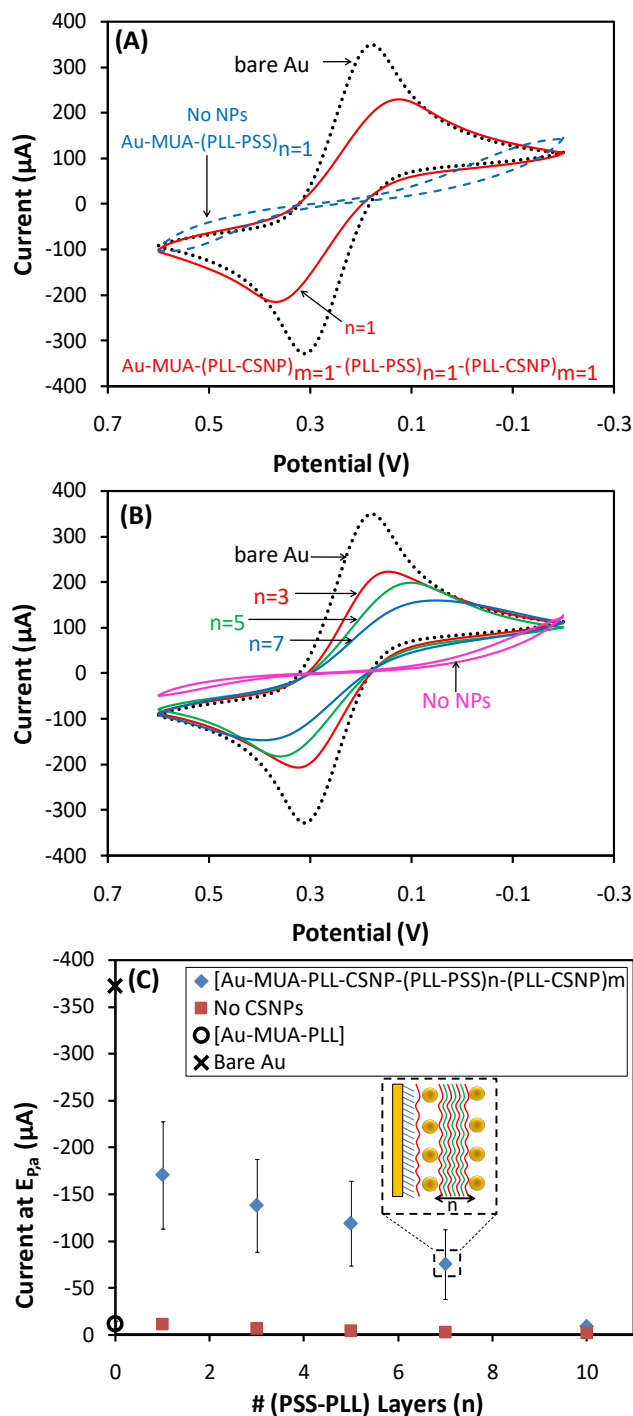


Figure 4. (A) Cyclic voltammetry of 5 mM ferricyanide in 0.5 M aqueous KCl supporting electrolyte (100 mV/sec) at a “double NP layer” hybrid PE-NP films of thickness $n=1$, for an overall film construction of $\text{Au-MUA-(PLL-CSNP)}_{m=1}\text{-(PLL-PSS)}_{n=1}\text{-(PLL-CSNP)}_{m=1}$. (B) Cyclic voltammetry of 5 mM ferricyanide in 0.5 M aqueous KCl supporting electrolyte (100 mV/sec) at a “double NP layer” hybrid PE-NP films where the number of PE bilayers (n) between NPs close to the electrode at the SAM/film interface and a terminal layer of NPs at the film/solution interface is systematically varied between 1 (Figure 4A) and 10 (Figure 4B), a film composition represented by $\text{Au-MUA-(PLL-CSNP)}_{m=1}\text{-(PLL-PSS)}_{n=1,3,5,7}\text{-(PLL-CSNP)}_{m=1}$. Each set of voltammograms (A,B) contains ferricyanide voltammetry at a bare gold electrode (black, dotted) as well as at a similar PE film constructed without NPs (“no NPs”). (C) Current measurements made at the anodic peak potential (E_{pa}) for ferricyanide as a function of PE bilayers (n) for these films constructed with and without NPs. For comparison, the anodic voltammetric current of ferricyanide at bare gold (\times) and at a gold electrode modified with MUA-PLL (\circ) are included at $n=0$. Error bars for the data representing films with no NPs are smaller than the data points themselves.

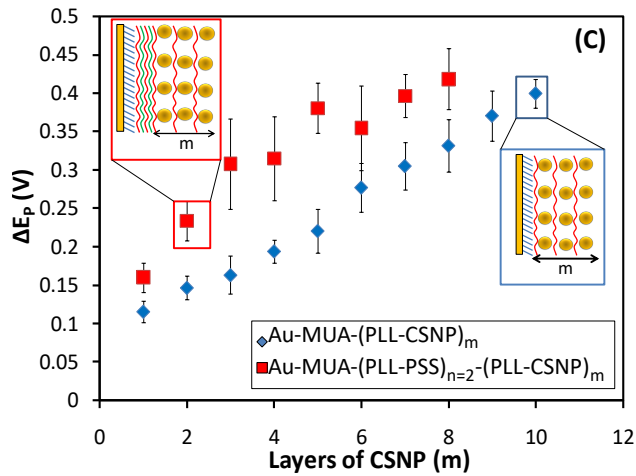
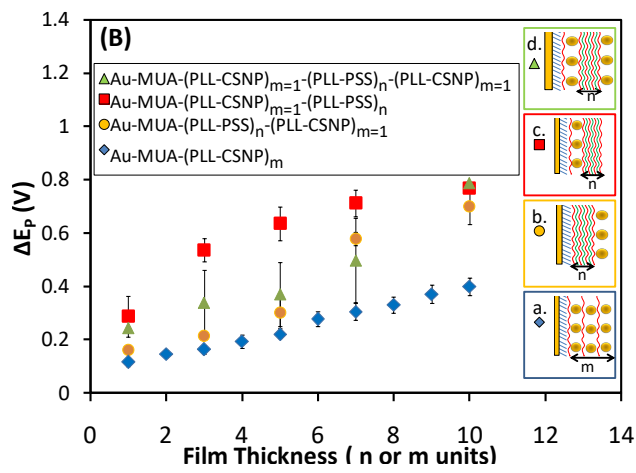
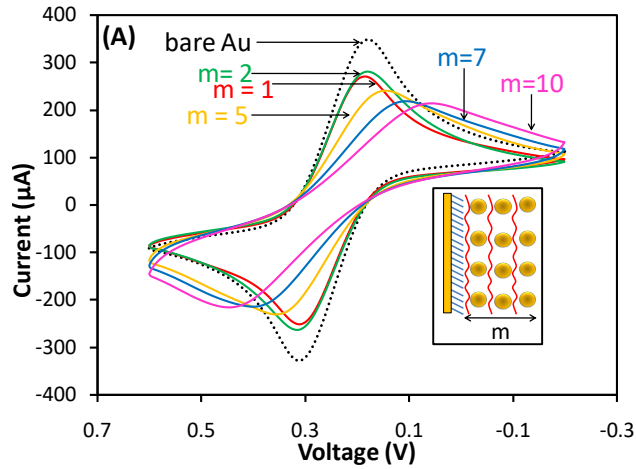


Figure 5. (A) Cyclic voltammetry of 5 mM ferricyanide in 0.5 M aqueous KCl supporting electrolyte (100 mV/sec) at multilayer CSNP films. In this case, the bare gold electrode (black, dotted) was modified with consecutive layers (m) of PLL-CSNPs from m=1 (red, solid) to m=10 (pink, solid), for an overall film construction of [Au-MUA-(PLL-CSNP)_{m=1-10}] (not all shown). (B) Graphical representation of ET kinetics in the form of voltammetric peak splitting (ΔE_p) in multi-layer films (system a), single layer NP films (system b), double layer NP films (system c), and inverted single layer NP films (system d), as a function of film thickness (n or m units). (C) Graphical representation of ΔE_p of the multi-layer NP system (blue diamonds) vs. the multi-layer NP system with the first two layers of CSNPs replaced with PSS polymer (red squares), plotted as a function of increasing layers of CSNPs (m).